

An incoherent feed-forward loop mediates robustness and tunability in a plant immune network

Akira Mine^{1,2}, Tatsuya Nobori^{1,†}, Maria C Salazar-Rondon^{1,†}, Thomas M Winkelmüller¹, Shajahan Anver¹, Dieter Becker¹ & Kenichi Tsuda^{1,*} 

Abstract

Immune signaling networks must be tunable to alleviate fitness costs associated with immunity and, at the same time, robust against pathogen interferences. How these properties mechanistically emerge in plant immune signaling networks is poorly understood. Here, we discovered a molecular mechanism by which the model plant species *Arabidopsis thaliana* achieves robust and tunable immunity triggered by the microbe-associated molecular pattern, flg22. Salicylic acid (SA) is a major plant immune signal molecule. Another signal molecule jasmonate (JA) induced expression of a gene essential for SA accumulation, *EDS5*. Paradoxically, JA inhibited expression of *PAD4*, a positive regulator of *EDS5* expression. This incoherent type-4 feed-forward loop (I4-FFL) enabled JA to mitigate SA accumulation in the intact network but to support it under perturbation of *PAD4*, thereby minimizing the negative impact of SA on fitness as well as conferring robust SA-mediated immunity. We also present evidence for evolutionary conservation of these gene regulations in the family *Brassicaceae*. Our results highlight an I4-FFL that simultaneously provides the immune network with robustness and tunability in *A. thaliana* and possibly in its relatives.

Keywords incoherent feed-forward loop; jasmonate; plant immunity; salicylic acid; signaling perturbation

Subject Categories Evolution; Immunology; Plant Biology

DOI 10.15252/embr.201643051 | Received 13 July 2016 | Revised 9 November 2016 | Accepted 8 December 2016 | Published online 9 January 2017

EMBO Reports (2017) 18: 464–476

Introduction

Proper processing of signals through signaling networks is central for organisms to respond accordingly to the signals. As such, signaling networks are comprised of recurring regulatory subnetwork structures called network motifs with various information-processing functions. Feed-forward loop (FFL), which consists of two regulators and

a target, represents a major class of network motifs [1]. Each of interactions among the components of a FFL can be either positive (activation) or negative (repression). As a result, there are eight possible structural configurations of FFL. Of these configurations, incoherent type-4 FFL (I4-FFL), in which a regulator has a positive effect on the target but a negative effect on the other regulator that positively regulates the target, is rare in biological networks and, therefore, its biological function has rarely been described.

In nature, plants are in constant contact with a wide variety of microbes, which often produce common molecular signatures known as microbe-associated molecular patterns (MAMPs) [2]. Plants sense MAMPs by plasma membrane-localized pattern recognition receptors and feed this information into signaling networks that finely control the output immune reaction designated as pattern-triggered immunity (PTI) [2–5]. Since recognized MAMPs are often common to a class of microbes [2], PTI could be triggered by both pathogenic and non-pathogenic microbes. Therefore, it is vital for plants to avoid unnecessary PTI against non-pathogenic microbes, as there is a trade-off between immunity and growth [6–9]. At the same time, it is important to retain PTI that is effective against pathogens that deploy virulence effectors to interfere with immune signaling components [10,11] and that can function under perturbation due to diverse environmental conditions [12]. The molecular mechanisms that allow these properties to emerge from PTI signaling networks are poorly understood.

Plants rely on PTI to resist necrotrophs that actively kill hosts to acquire nutrients as well as to resist biotrophs that require living hosts for multiplication [2,13]. The phytohormone jasmonate (JA) is a major contributor to immunity against necrotrophs [13]. JA is produced in response to MAMPs such as flg22 [14] and chitin [15], a part of bacterial flagellin and a part of fungal cell walls, respectively. JA biosynthesis requires allene oxide synthase encoded by *DELAYED-DEHISCENCE 2 (DDE2)* [16]. JA and its derivatives including methyl JA (MeJA) can be converted to JA-isoleucine (JA-Ile) [17,18]. Perception of JA-Ile by the F-box protein CORONATINE INSENSITIVE 1 (COI1) leads to ubiquitination- and proteasome-dependent degradation of JASMONATE ZIM DOMAIN

¹ Department of Plant Microbe Interactions, Max Planck Institute for Plant Breeding Research, Cologne, Germany

² Center for Gene Research, Nagoya University, Chikusa-Ku, Nagoya, Japan

*Corresponding author. Tel: +49 221 5062 302; E-mail: tsuda@mpipz.mpg.de

[†]These authors contributed equally to this work

(JAZ) proteins [19–21]. This liberates downstream transcription factors including MYC2 and its homologues MYC3 and MYC4, which are normally repressed by JAZ proteins in the resting state, thereby activating JA-mediated transcriptional responses and immunity [22,23].

Another phytohormone, salicylic acid (SA), is a central regulator of immunity against biotrophs and hemi-biotrophs such as the bacterial pathogen *Pseudomonas syringae* [13,24]. Indeed, SA production is activated by the bacterial MAMP flg22 [25]. Previous studies have identified a number of genes involved in SA biosynthesis and signaling. *SALICYLIC ACID-INDUCTION DEFICIENT 2 (SID2)* encodes an isochorismate synthase that is essential for SA biosynthesis through the isochorismate pathway [26]. *PHYTOALEXIN-DEFICIENT 4 (PAD4)* contributes to MAMP-induced SA accumulation [25,27]. *ENHANCED DISEASE SUSCEPTIBILITY 5 (EDS5)* is essential for pathogen-induced SA accumulation in *Arabidopsis thaliana* [28–30] and encodes a MATE transporter, which was proposed to mediate SA transport from chloroplasts, the site of SID2-mediated SA biosynthesis, to the cytoplasm [30]. SA affects transcriptional regulation of hundreds of genes, including *PATHOGENESIS-RELATED 1 (PR1)* [31]. SA accumulation and signaling should be tightly controlled, as excessive activation of SA biosynthesis or signaling is associated with growth retardation [6,32–34]. However, current understanding of the signaling mechanisms regulating SA production is fragmented.

Phytohormone signaling pathways form a complex network, which could confer great regulatory potential to control plant responses to diverse internal and external stimuli [35,36]. For instance, antagonism between JA and SA is thought to be important to activate proper immunity depending on pathogen lifestyles [13,37]. Interestingly, cooperation between JA and SA has been also reported [14,38]. Thus, plants appear to have context-dependent crosstalk between JA and SA. However, the molecular mechanisms and the biological relevance of the JA–SA crosstalk remain elusive.

Previously, a quantitative model was built to capture signal flows in the network consisting of the JA, SA, PAD4, and ethylene (ET) signaling sectors during PTI [14]. The model pointed to JA and PAD4 as the sole determinants of SA signaling activity [14]. Here, we report the molecular mechanism by which JA enables robust and tunable SA accumulation during PTI in *A. thaliana*. Our data demonstrate that JA inhibits expression of PAD4, a positive regulator of EDS5 expression. Paradoxically, JA induces EDS5 expression directly via the transcription factor MYC2. This I4-FFL explains the negative role of JA on SA accumulation in the intact network and its positive role in the absence of PAD4. We also show that both of these transcriptional effects of JA occur not only in *A. thaliana* but also in other *Brassicaceae* species. Taken together, our results highlight the I4-FFL that allows plants to alleviate the negative impact of SA on fitness as well as to support robust SA accumulation when PAD4 function is compromised.

Results

JA is defined as a repressor or activator of SA accumulation depending on PAD4

To investigate the regulatory relationship between JA and PAD4 in MAMP-triggered SA accumulation, we measured SA levels in

leaves of wild-type, *dde2*, *pad4*, and *dde2 pad4* plants after infiltration with flg22. In the wild type, an increase in SA level was observed at 9 h post-infiltration (Fig 1A). The SA level was elevated in *dde2*, which is reminiscent of the often described repressive effect of JA on SA. In contrast, in *pad4*, SA was increased by flg22 treatment, but to a level lower than in wild type, which is consistent with PAD4 being a positive regulator of SA accumulation in response to flg22 [25]. Strikingly, flg22-triggered SA accumulation was abolished in *dde2 pad4*, showing a requirement of JA for SA induction in the absence of PAD4. Similar patterns were observed for expression of the canonical SA marker gene *PR1* (Fig 1B), as well as that of *At2g26400* and *At2g30550* (Fig 1C and D), which was shown to be induced upon challenge with *P. syringae* pv. *tomato* DC3000 (*Pto*) in an SA-dependent manner [39]. In line with the previous study [14], these results demonstrated that JA acts as a repressor or activator of SA accumulation in the presence or absence of PAD4, respectively, during flg22-triggered PTI.

JA represses PAD4 expression through the action of MYC transcription factors

Since the enhanced SA accumulation in *dde2* was dependent on PAD4 (Fig 1A; compare *dde2* and *dde2 pad4*), we tested whether JA represses PAD4 expression. PAD4 expression was elevated in *dde2* as well as in *coi1* at 9 h after flg22 treatment (Fig 2A). The transcription factors MYC2 and its homologues MYC3 and MYC4 are important for transcriptional responses to JA, and we found a MYC2-binding motif (G box; CACATG) in the PAD4 promoter using the online tool Athena (Fig 2B) [40–42]. These observations led us to test whether MYC2 and its homologues MYC3 and MYC4 are responsible for JA-mediated repression of PAD4 expression. Indeed, increased expression of PAD4 was observed in *myc2 myc3 myc4* but not in *myc2* (Fig 2A). Thus, these MYCs seem to act redundantly to repress PAD4 expression during flg22-triggered PTI.

We then tested whether MYC2 directly binds to the G box motif in the PAD4 promoter in planta by chromatin immunoprecipitation (ChIP) using a transgenic *A. thaliana* line constitutively expressing the MYC2-GFP fusion protein (Fig EV1). The enrichment of the G box sequence in immunoprecipitates from MYC2-GFP plants relative to those from wild-type plants was determined by qPCR. A DNA segment from the coding sequence (CDS) of PAD4 was used as a negative control. Although these MYC transcription factors contribute to PAD4 repression (Fig 2A), we did not observe direct binding of MYC2 to the PAD4 promoter even after the treatment with flg22 or MeJA (Fig 2C and D). Considering that MYC2, MYC3, and MYC4 are transcriptional activators with shared DNA-binding specificity [43], it is likely that these MYC transcription factors indirectly repress PAD4 expression through an intermediate factor(s).

JA induces EDS5 expression directly through MYC2

Since JA positively contributes to SA accumulation in the absence of PAD4, we examined expression levels of SID2 and EDS5, both of which are essential for pathogen-induced SA accumulation [25,26,28,29]. At 5 h after flg22 treatment, expression of SID2 was similar in *pad4* and *dde2 pad4* (Fig 3A). In contrast, expression of

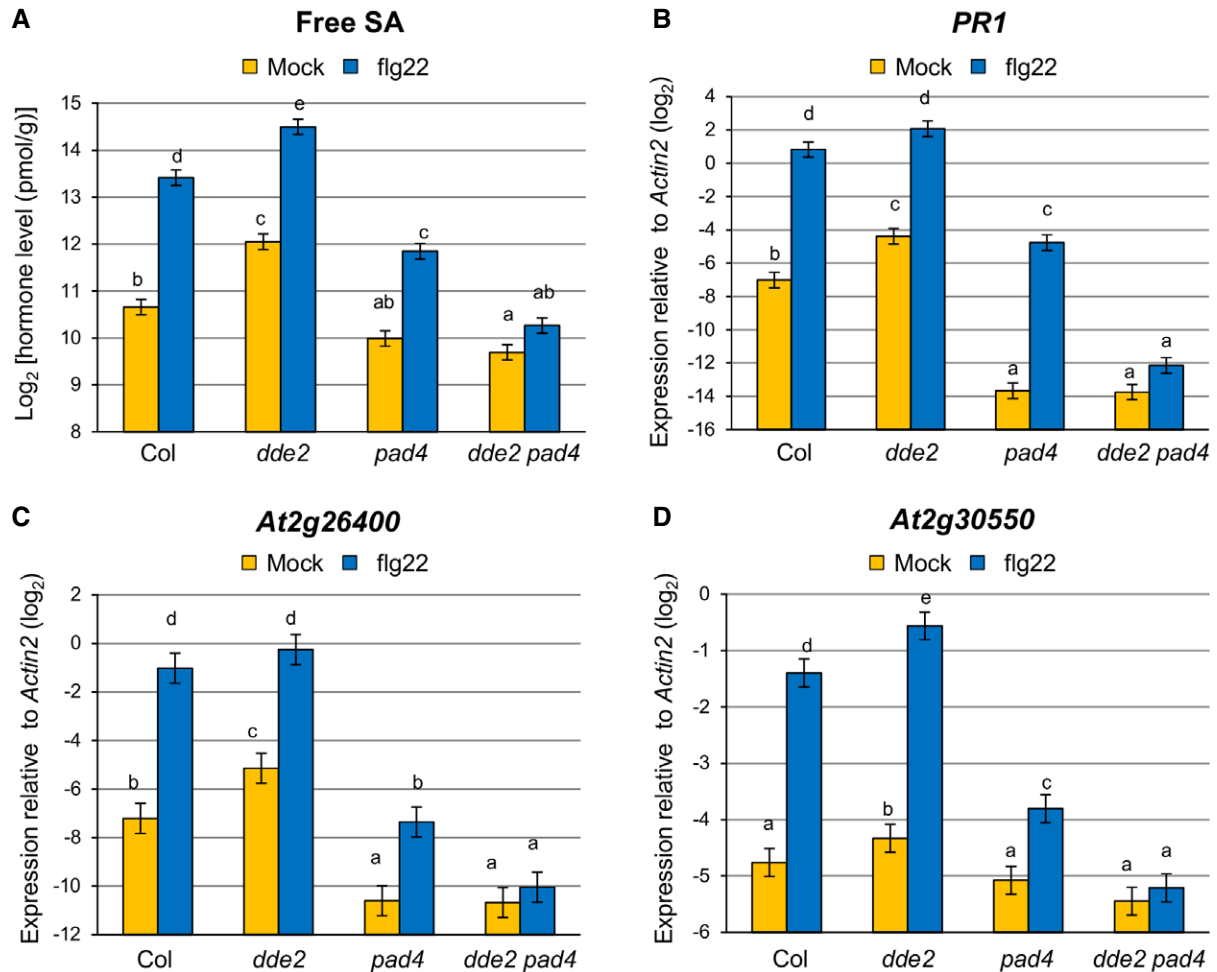


Figure 1. JA is genetically defined as a repressor or activator of SA accumulation depending on PAD4.

A Measurement of SA levels in leaves infiltrated with water (mock) or 1 μ M flg22 at 9 hpi. Bars represent means and standard errors of the SA levels on a log₂ scale calculated from two independent experiments using a mixed linear model.

B–D RT-qPCR analysis of *PR1*, *At2g26400* and *At2g30550* expression in leaves infiltrated with water (mock) or 1 μ M flg22 at 9 hpi. Bars represent means and standard errors of the log₂ expression level relative to *Actin2* (*At3g18780*) calculated from three independent experiments using a mixed linear model.

Data information: The Benjamini–Hochberg method was used to adjust *P*-values (two-tailed *t*-tests) for correcting multiple hypothesis testing. Statistically significant differences are indicated by different letters (adjusted *P*-value < 0.05).

EDS5 was significantly lower in *dde2 pad4* than in *pad4*, and *EDS5* induction was abolished in *dde2 pad4* (Fig 3B), indicating that *PAD4* and JA together are responsible for flg22-triggered *EDS5* expression. Importantly, the compromised *EDS5* induction in *dde2 pad4* was correlated well with the compromised SA induction in *dde2 pad4* (Fig 1A), suggesting that *EDS5* is the causal gene for the positive role of JA in SA accumulation.

To explore the mechanism by which JA regulates *EDS5* expression, the promoter sequence of *EDS5* was searched for *cis* elements using the Athena analysis tool. We found a canonical G box (CACGTG), the binding site for MYC transcription factors, in close proximity to the transcription start site of *EDS5* (Fig 3D). This prompted us to test whether MYC2 and its homologues MYC3 and MYC4 are responsible for *EDS5* induction by JA. In the wild-type plants, MeJA treatment induced *EDS5* expression at the three time points tested, while *EDS5* expression was significantly reduced in

myc2 and *myc2 myc3 myc4* (Fig 3C), demonstrating that these MYCs are required for JA-mediated *EDS5* induction. We then performed ChIP experiments using MYC2-GFP plants treated with or without flg22 or MeJA to test whether MYC2 directly binds to the *EDS5* promoter. We found a significant enrichment of the promoter sequence containing the G box motif in all the conditions tested, but no enrichment was observed for a DNA segment in the CDS of *EDS5* used as a negative control (Fig 3E and F). To test whether the G box in the *EDS5* promoter is required for MYC2-mediated transcriptional activation of *EDS5*, we carried out luciferase (Luc) reporter assays using *Arabidopsis* protoplasts. Expression of MYC2 significantly induced the wild-type *EDS5* promoter-driven Luc activity, whereas deletion of the G box abolished this MYC2-mediated transcriptional activation (Fig 3G). Taken together, these results indicate that MYC2 directly binds to the *EDS5* promoter and controls *EDS5* induction by JA.

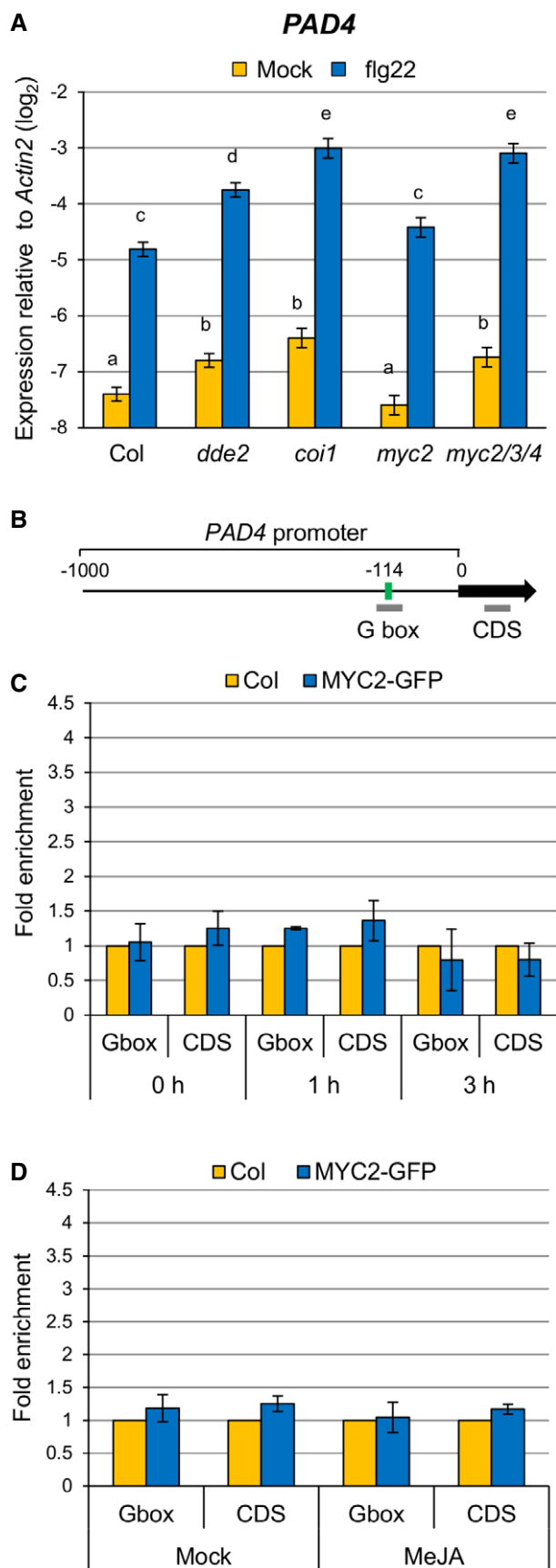


Figure 2. JA represses *PAD4* expression through MYC transcription factors.

A RT-qPCR analysis of *PAD4* expression in leaves infiltrated with water (mock) or 1 μ M flg22 at 9 hpi. Bars represent means and standard errors of the log₂ expression level relative to *Actin2* calculated from four independent experiments using a mixed linear model.

B *PAD4* promoter showing the G box motif located 114 bp upstream of the transcription start site. Bold gray horizontal lines show the regions amplified by different qPCR primers.

C, D ChIP-qPCR analysis of MYC2 binding to the *PAD4* promoter. MYC2-GFP seedlings were treated with 1 μ M flg22 for the indicated time periods (**C**) or 100 μ M MeJA for 3 h (**D**). Bars represent means and standard errors of the fold enrichment relative to the wild-type plants set to 1, calculated from two independent experiments.

Data information: In (**A**), the Benjamini–Hochberg method was used to adjust *P*-values (two-tailed *t*-tests) for correcting multiple hypothesis testing and statistically significant differences are indicated by different letters (adjusted *P*-value < 0.05).

Reconstitution of *EDS5* expression restores flg22-triggered SA accumulation and immunity in *dde2 pad4*

To test for a causal link between JA-mediated *EDS5* expression and SA accumulation, we generated transgenic lines expressing *EDS5* under two different promoters in *dde2 pad4*. In two independent lines expressing *EDS5* from the constitutive 35S promoter, *EDS5* expression was higher than in the wild type and was not altered after flg22 treatment (Fig 4A). The expression level of *EDS5* was more than eightfold higher in *p35S:EDS5* line #1 than in line #2 (Fig 4A). Another transgenic line expressing *EDS5* from the *SID2* promoter showed the wild-type level of *EDS5* expression after mock treatment and slightly higher expression of *EDS5* compared to the wild type after flg22 treatment (Fig 4A). This is in accordance with our finding that *SID2* was responsive to flg22 in *dde2 pad4* (Fig 3A). Induction of SA accumulation and *PR1* expression by flg22 was detected in *p35S:EDS5* line #1 but not in line #2 (Fig 4B and C). The *pSID2:EDS5* line also showed restored SA accumulation and *PR1* expression after flg22 treatment (Fig 4B and C) although the expression level of *EDS5* was lower than in *p35S:EDS5* line #2. Thus, a minimal level of *EDS5* expression, which is not achieved in *dde2 pad4*, is required for flg22-triggered SA accumulation. These results also suggest that transcriptional induction of *EDS5* in response to flg22 can overcome the need to constitutively express *EDS5* at a very high level for flg22-triggered SA accumulation. As *EDS5* is inducible by flg22, this transcriptional induction might be a critical part of flg22-triggered SA accumulation. Overall, our data clearly established a causal connection between compromised *EDS5* expression or induction and the compromised SA accumulation in *dde2 pad4* in response to flg22.

To test whether the restored SA accumulation in the transgenic lines is relevant for immunity, we measured *Pto* growth. Leaves were co-infiltrated with *Pto* and flg22 and sampled at 2 days after infiltration. Co-infiltration of flg22 inhibited *Pto* growth in the wild type but not in *fls2*, a mutant lacking the receptor for flg22 (Fig 4D). This reduction in bacterial growth, termed flg22-triggered PTI, was calculated by subtracting the log₁₀-transformed bacterial titer in flg22-treated leaves from that in mock-treated leaves. Flg22-triggered PTI was much less in *dde2 pad4* than in the wild

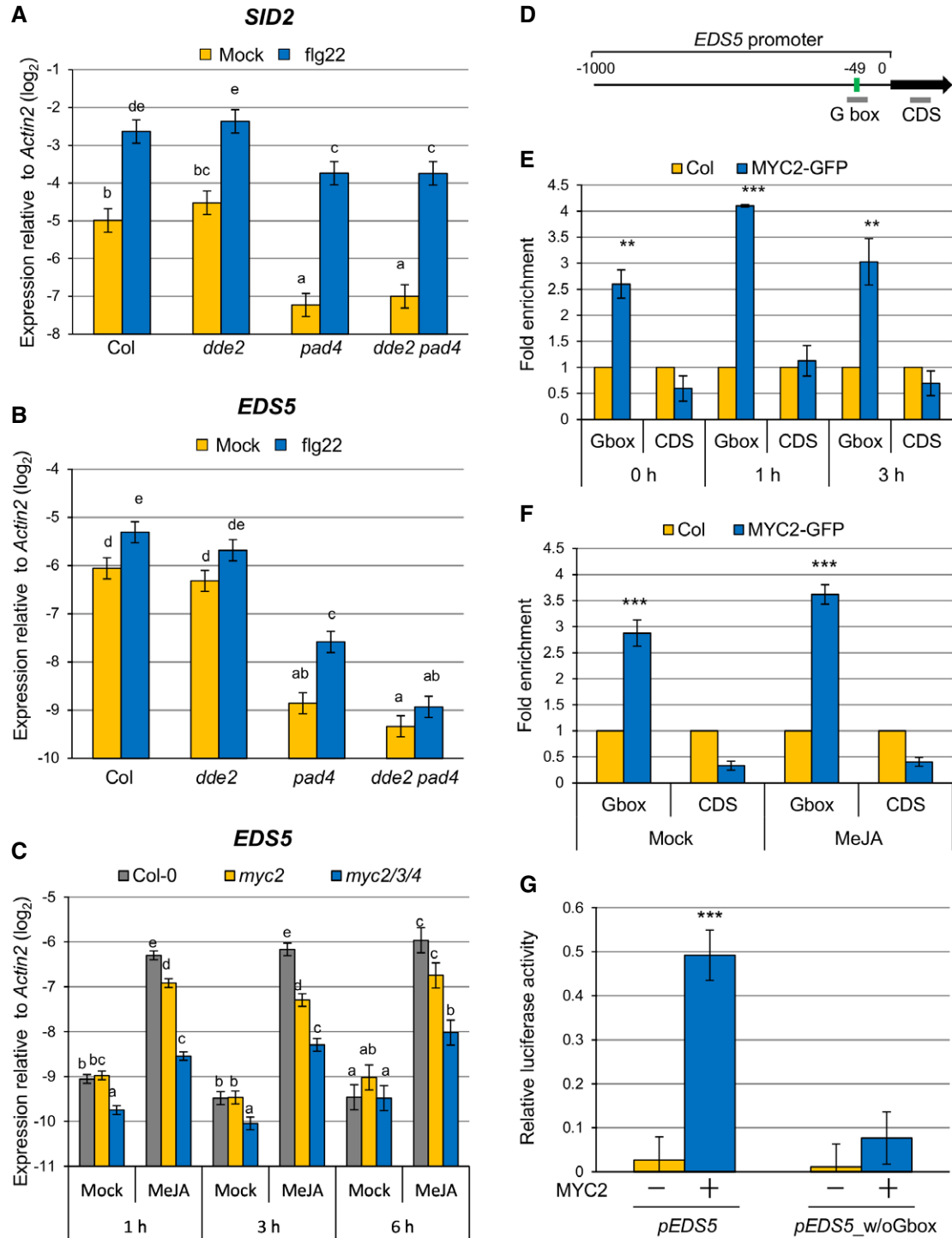


Figure 3.

type. Importantly, flg22-triggered PTI was significantly higher in the transgenic lines with restored SA accumulation than in *dde2 pad4* plants (Fig 4D). Given the genetic requirement for JA in flg22-triggered *EDS5* expression and SA accumulation in *pad4* (Figs 1A and 3B), we conclude that JA enables robust flg22-triggered PTI by supporting SA accumulation through MYC2-activated *EDS5* expression.

Distinct effects of JA on bacterial resistance depending on *PAD4*

Our genetic perturbation and reconstitution approach illustrates an I4-FFL consisting JA (MYC transcription factors), *PAD4*, and *EDS5* (Fig 5A). To further investigate the roles of the I4-FFL in plant immunity, we assessed effects of exogenous MeJA application on flg22-triggered PTI against *Pto* in the wild type, *dde2 pad4*, and the

Figure 3. MYC2 directly regulates EDS5 induction by JA.

- A, B RT-qPCR analysis of *SID2* (A) and *EDS5* (B) expression in leaves infiltrated with water (mock) or 1 μ M flg22 at 5 hpi. Bars represent means and standard errors of the log₂ expression levels relative to *Actin2* calculated from four independent experiments using a mixed linear model.
- C RT-qPCR analysis of *EDS5* expression in seedlings treated with water (mock) or 100 μ M MeJA for the indicated time periods. Bars represent means and standard errors of the log₂ expression level relative to *Actin2* calculated from two independent experiments using a mixed linear model.
- D *EDS5* promoter showing the G box motif located 49 bp upstream of the transcription start site. Bold gray horizontal lines show the regions amplified by different qPCR primers.
- E, F ChIP-qPCR analysis of MYC2 binding to the *EDS5* promoter. MYC2-GFP seedlings were treated with 1 μ M flg22 for the indicated time periods (E) or 100 μ M MeJA for 3 h (F). Bars represent means and standard errors of the fold enrichment relative to the wild-type plants set to 1, calculated from two independent experiments.
- G Luciferase reporter assays using *EDS5* promoters with or without G box. Luc reporter construct driven by the wild-type *EDS5* promoter (*pEDS5*) or the *EDS5* promoter without G box (*pEDS5_w/oGbox*) was transfected with or without 35S-MYC2 plasmid to *Arabidopsis* protoplasts. Bars represent means and standard errors of the Luc activity relative to the internal control (Luc derived from *Renilla* spp. driven by 35S promoter) calculated from three independent experiments each with three biological replicates.

Data information: In (A–C), the Benjamini–Hochberg method was used to adjust *P*-values (two-tailed *t*-tests) for correcting multiple hypothesis testing. Two groups not sharing any letters show statistically significant differences (adjusted *P*-value < 0.05). In (E–G), asterisks indicate statistically significant differences from the wild type (E, F) or from the empty vector control (G) (***P* < 0.01, ****P* < 0.001; two-tailed *t*-tests).

transgenic *p35S:EDS5 #1* and *pSID2:EDS5* lines with restored flg22-triggered SA accumulation. MeJA reduced flg22-triggered PTI in the wild type but enhanced it in *dde2 pad4* (Fig 5B), demonstrating that the negative effect of JA is dominant in the presence of *PAD4*, whereas the positive effect of JA is evident in the absence of *PAD4*. MeJA had no effect on flg22-triggered immunity in the transgenic lines, suggesting that the positive role of JA in the absence of *PAD4* is to support SA accumulation via *EDS5* expression. These results are consistent with our I4-FFL model, in which JA negatively or positively regulates SA-mediated bacterial resistance in the presence or absence of *PAD4*, respectively.

PAD4-regulated signaling to SA activation is perturbed at high temperature such as 28°C [44]. To investigate the biological importance of the I4-FFL in a more natural context, we measured *Pto* growth in the wild type, *dde2*, *pad4*, and *dde2 pad4* at 22°C and 28°C. As shown in Fig 5C, *pad4* was more susceptible to *Pto* than the wild type at 22°C. Such enhanced susceptibility of *pad4* was not observed at 28°C, indicating that *PAD4* function in *Pto* resistance is compromised at this temperature. Interestingly, *dde2* and *dde2 pad4* supported more *Pto* growth than the wild type and *pad4*, respectively, at 28°C. No significant differences in *Pto* growth between Col and *dde2* and between *pad4* and *dde2 pad4* were observed at 22°C. The effects of *dde2* mutation at 22°C might be masked by coronatine produced by *Pto*, which activates JA signaling by acting as a molecular mimic of JA-Ile [20,45]. Overall, these results support a biological significance of the I4-FFL for conferring JA-mediated bacterial resistance under perturbation of *PAD4* at high temperature, which can naturally occur.

Conservation and diversification of JA-mediated regulation of *PAD4* and *EDS5* in *Brassicaceae*

The importance of the I4-FFL identified in this study could be reflected by evolutionary conservation in plants. To address this point, we used the *A. thaliana* *EDS5* protein sequence to identify related proteins in some *Brassicaceae* species, tomato and rice whose genome sequences and gene annotations are available. Construction of a phylogenetic tree using the related proteins suggests that the *EDS5* clade is conserved in the family *Brassicaceae* but not in other plants (Fig EV2). Since our results suggest that MYC2 controls JA-mediated *EDS5* induction through binding to the

CACGTG G box motif (Fig 3E–G), we surveyed 500 bp upstream of the transcription start sites (hereafter referred to as “promoters”) and 5'-UTRs of these *EDS5* orthologues for this motif. Interestingly, the G box motif was found in the *EDS5* promoters of *A. thaliana*, *Arabidopsis lyrata*, *Capsella grandiflora*, and *Eutrema salsugineum*, whereas it was located in the 5'-UTRs in *Capsella rubella* and *Brassica rapa* (Fig EV3). MeJA treatment induced *EDS5* expression in *A. thaliana*, *A. lyrata*, and *E. salsugineum*, but not in *C. rubella* (Fig 6A). This is in line with the presence or absence of the G box motif in the promoters. *Capsella rubella* was responsive to MeJA in other ways, as exemplified by induction of a homologue of the *A. thaliana* *VSP2*, a JA responsive gene (Fig EV4). The inducibility of *EDS5* by JA is not correlated to the phylogenetic distance within *Brassicaceae* [46]. Thus, these results may suggest that the JA-mediated *EDS5* regulation emerged in the ancestor of *Brassicaceae* and *C. rubella* has lost it.

PAD4 is conserved among flowering plants [47]. We therefore tested whether JA-mediated repression of *PAD4* expression is conserved among *Brassicaceae*. *A. thaliana*, *A. lyrata*, *C. rubella*, and *E. salsugineum* plants were treated with mock or MeJA, followed by flg22 treatment. In *A. thaliana*, MeJA treatment had no effect on *PAD4* expression but inhibited *PAD4* induction by flg22 (Fig 6B). As in *A. thaliana*, MeJA had an inhibitory effect on *PAD4* induction by flg22 in the other three species (Fig 6B). Thus, the repressive effect of JA on *PAD4* expression during flg22-PTI appears to be conserved in *Brassicaceae*.

Discussion

It is vital for plants to invoke robust immunity against pathogens that interfere with immune signaling and, at the same time, to minimize fitness costs associated with immunity. This is particularly relevant to PTI, since it is activated by MAMPs which do not distinguish pathogens from other beneficial or benign microbes. In this study, we identified an I4-FFL consisting of JA, *PAD4*, and *EDS5* in the PTI signaling network in *A. thaliana*. JA induces *EDS5* expression directly via the transcription factor MYC2 while repressing expression of *PAD4* which positively contributes to *EDS5* expression. I4-FFL is rare in biological networks and, therefore, its biological function has rarely been characterized [48,49]. In the context of PTI,

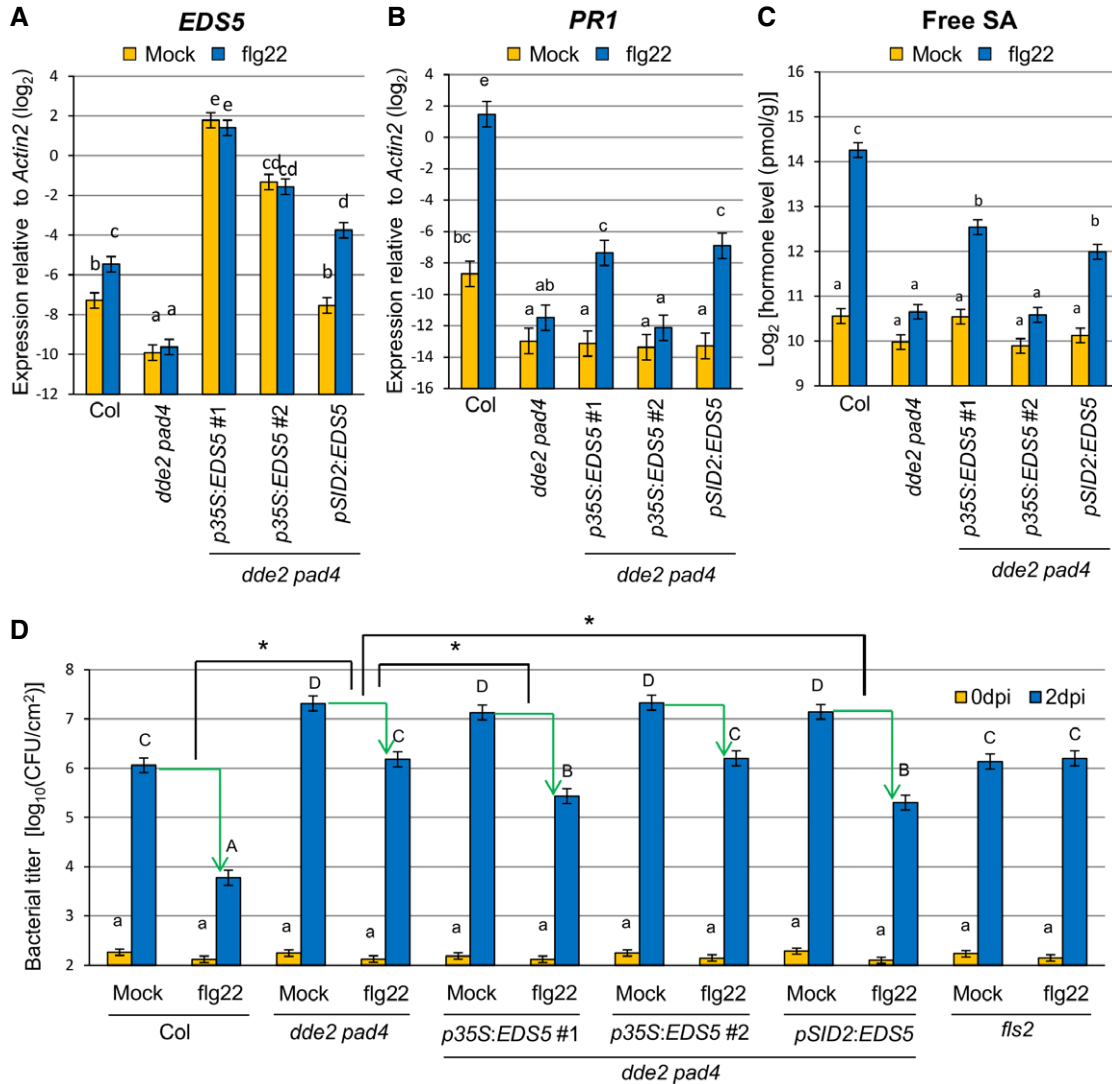


Figure 4. Reconstitution of *EDS5* expression restores fig22-triggered SA accumulation and fig22-PTI in *dde2 pad4*.

A, B RT-qPCR analysis of *EDS5* (A) and *PR1* (B) expression in leaves of Col, *dde2 pad4*, *p35S::EDS5* lines and a *pSID2::EDS5* line infiltrated with water (mock) or 1 μM fig22. The expression levels of *EDS5* and *PR1* were measured at 5 hpi and 9 hpi, respectively. Bars represent means and standard errors of the log₂ expression levels relative to *Actin2* calculated from two independent experiments using mixed linear models.

C Measurement of SA levels in leaves of Col, *dde2 pad4*, *p35S::EDS5* lines and a *pSID2::EDS5* line infiltrated with water (mock) or 1 μM fig22 at 9 hpi. The means and standard errors calculated from two independent experiments using a mixed linear model are shown on a log₂ scale.

D Bacterial growth assay in leaves of Col, *dde2 pad4*, *p35S::EDS5* lines and a *pSID2::EDS5* line infiltrated with *Pto* (OD₆₀₀ = 0.0002) together with water (mock) or 1 μM fig22. The bacterial titers at 0 or 2 dpi were measured. Bars represent means and standard errors of two independent experiments with at least 4 or 12 biological replicates for 0 dpi or 2 dpi in each experiment, respectively.

Data information: In (A–D), the Benjamini–Hochberg method was used to adjust *P*-values (two-tailed *t*-tests) for correcting multiple hypothesis testing. Two groups not sharing any letters show statistically significant differences (adjusted *P*-value < 0.05). In (D), asterisks indicate statistically significant differences of the differences (adjusted *P*-value < 0.05).

PAD4 repression by JA is functionally dominant in the intact network of wild-type plants, which explains reduction in SA accumulation in *pad4* and increase in *dde2*. However, in the absence of *PAD4*, the positive contribution of JA to SA accumulation becomes apparent. Consistently, SA induction in response to fig22 was abolished in *dde2 pad4*. The JA-mediated suppression of *PAD4* expression is likely important to alleviate the negative impact of SA on plant growth [6,32–34]. In contrast, the JA-mediated *EDS5*

induction provides robust SA accumulation in fig22-triggered immunity when *PAD4* cannot fulfill its function, for example, due to pathogen effectors or environmental factors.

A mechanism by which JA inhibits SA accumulation was uncovered by characterizing the mode of action of the JA-mimicking bacterial phytotoxin coronatine produced by *P. syringae* [50]. It was demonstrated that MYC2 transcriptionally activates the NAC (petunia NAM and *Arabidopsis* ATAF1, ATAF2, and CUC2) transcription

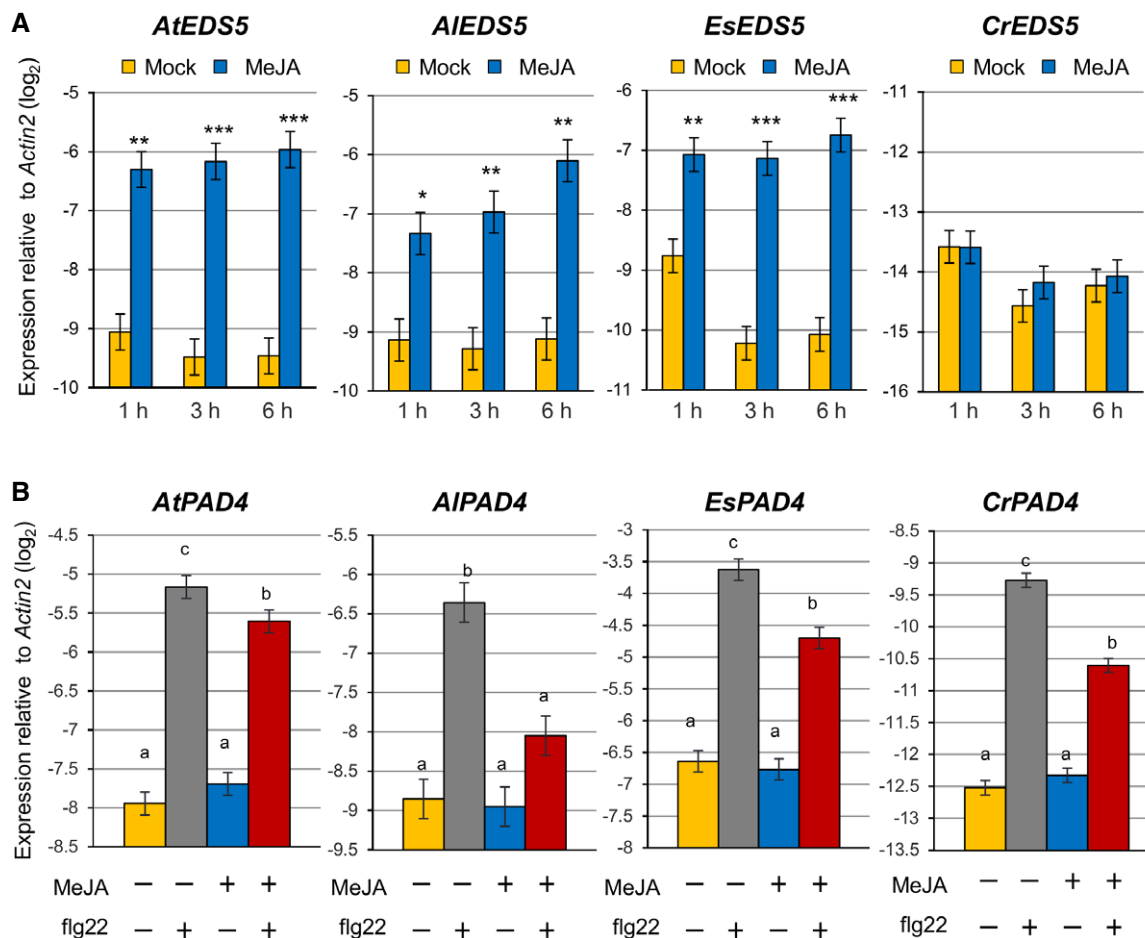


Figure 6. Conservation and diversification of the transcriptional regulation of *EDS5* and *PAD4* by JA in Brassicaceae.

A, B RT-qPCR analysis of *EDS5* (A) and *PAD4* (B) expression in seedlings of *Arabidopsis thaliana*, *Arabidopsis lyrata*, *Capsella rubella*, and *Eutrema salsugineum*. In (A), seedlings were treated with mock (water) or MeJA (100 μ M) for the indicated time periods. Asterisks indicate statistically significant differences from the mock controls at each time point (* P < 0.05, ** P < 0.01, *** P < 0.001; two-tailed t-tests). In (B), seedlings were treated with mock (water) or MeJA (100 μ M) for 3 h, followed by treatment with mock (water) or flg22 (1 μ M) for 30 min. The Benjamini-Hochberg method was used to adjust P -values (two-tailed t-tests) for correcting multiple hypothesis testing, and statistically significant differences were indicated by different letters (adjusted P -value < 0.05). Bars represent means and standard errors of the \log_2 expression levels relative to *Actin2* calculated from two independent experiments using mixed linear models.

in which *PAD4* function is perturbed by environmental factors such as high temperature and likely by pathogen effectors. With respect to the latter situation, it is noteworthy that some bacterial effectors target *EDS1*, which is required for *PAD4* function [51,52].

It would be interesting to discuss effects of coronatine in the framework of the I4-FFL identified in this study. Coronatine is a JA-mimicking virulence factor that suppresses SA-mediated immunity to promote bacterial growth [20,45,50]. Consistently, we observed that MeJA treatment after flg22 infiltration promotes *Pto* growth in the wild type. However, in *dde2 pad4*, MeJA treatment reduced *Pto* growth. Thus, coronatine may have a negative impact on bacterial virulence when combined with other effectors that interfere with *PAD4* activity as well as under environmental conditions in which *PAD4* cannot fulfill its function.

Although *A. thaliana* is an excellent model system to study molecular and genetic aspects of plant biology, it is becoming

increasingly important to expand our knowledge to other plant species [46]. In this study, we took advantage of the family Brassicaceae, to which *A. thaliana* belongs, for studying evolutionary conservation of the gene regulation that we identified in *A. thaliana*. Our results indicate that the repressive effect of JA on *PAD4* expression during PTI is conserved not only in *A. lyrata* and *C. rubella*, close relatives of *A. thaliana*, but also in *E. salsugineum*, a relatively phylogenetically distant species from *A. thaliana*. Thus, the repression of *PAD4* by JA may be a common regulatory mechanism for tunable SA accumulation during PTI in Brassicaceae. Since *PAD4* is conserved in flowering plants [47], it would be interesting to test whether JA represses *PAD4* expression during PTI in plant species outside Brassicaceae.

In contrast to *PAD4*, our phylogenetic analysis highlighted a Brassicaceae-specific clade to which *A. thaliana* *EDS5* belongs, suggesting that the role of *EDS5* in SA accumulation might be restricted to this family. Interestingly, our gene expression data

together with promoter analysis pointed to a good correlation between the presence or absence of the CACGTG G box motif in the promoters and the inducibility of *EDS5* by JA in *Brassicaceae*. We note that in *C. rubella*, in which JA does not induce *EDS5*, the CACGTG sequence is present downstream of the transcription start site and transcribed as a part of the 5'-UTR [53]. Thus, *C. rubella* might have lost JA-mediated *EDS5* induction by changing the transcription start site. This might also hold true for *B. rapa*, as the G box motif is located in the 5'-UTR (*Brassica rapa* FPsc v1.3, DOE-JGI, <http://phytozome.jgi.doe.gov/>). Overall, our comparative analysis suggests that *EDS5* and its transcriptional regulation by JA are an innovation of the family *Brassicaceae*.

In conclusion, our results highlight an I4-FFL that simultaneously provides robust and tunable regulation of SA response during PTI in *A. thaliana*. The transcriptional effects of JA on *EDS5* and *PAD4* appear to be highly conserved in the family *Brassicaceae*. Whether or not this reflects evolutionary conservation of the I4-FFL deserves further study.

Materials and Methods

Plant materials and growth conditions

Arabidopsis plants were grown in a chamber at 22°C with a 10-h light period and 60% relative humidity for 3 weeks and then in another chamber at 22°C with a 12-h light period and 60% relative humidity. The *A. thaliana* accession Col-0 was the background of all *Arabidopsis* mutants used in this study. *Arabidopsis dde2-2* [16], *pad4-1* [27], *dde2-2 pad4-1* [54], *coi1-1* [19], *jin1-9/myc2* (SALK_017005) [55], *myc2 myc3 myc4* [43], and *fls2* (SAIL_691C4) [56] were described previously. The MYC2-GFP overexpression plants were obtained from Dr. Hironaka Tsukagoshi (Meijo University, Japan). Seedlings of *A. thaliana*, *A. lyrata* (MN47), *C. rubella* (N22697), and *E. salsugineum* (Shandong) were grown on solidified half-strength Murashige and Skoog (MS) medium supplemented with 1% sucrose under a 10-h light period at 22°C.

Chemicals

MeJA (392705) and flg22 were purchased from Sigma (Munich, Germany) and EZBiolab Inc. (Westfield, IN, USA), respectively.

Cloning and plant transformation

The coding sequence (without introns) of *EDS5* (AT4G39030) was amplified by PCR using PrimeSTAR HS DNA polymerase (Takara-Clontech, Saint-Germain-en-Laye, France) and cloned into the pENTR/D-TOPO vector following the manufacturer's protocol (Life Technologies, Darmstadt, Germany) to generate pENTR_EDS5. The promoter sequence of *SID2* (*At1g74710*) [57] and the Nos terminator sequence from pER8 [58] were amplified by PCR and cloned into the NotI and AscI sites of pENTR_EDS5, respectively, to generate pENTR_pSID2_EDS5_Nos. pENTR_EDS5 and pENTR_pSID2_EDS5_Nos were then recombined into the Gateway-compatible binary vectors pFAST-R02 [59] and pFAST-R01 [59], respectively, through the LR reaction (Invitrogen). Primers used are listed in Appendix Table S1. All plasmids constructed in this study were verified by sequencing. *Arabidopsis*

thaliana dde2 pad4 plants were transformed using *Agrobacterium tumefaciens* strain GV3101 as described [16].

Statistical analysis

Statistical analysis was performed using the mixed linear model function, lmer, implemented in the package lme4 in the R environment. When appropriate, raw data were log-transformed to meet the assumptions of the mixed linear model. For the *t*-tests, the standard errors were calculated using the variance and covariance values obtained from the model fitting. The Benjamini–Hochberg methods were applied to correct for multiple hypothesis testing when all pairwise comparisons of the mean estimates were made in a figure.

RNA extraction, cDNA synthesis, and quantitative PCR

Leaves of 4- to 5-week-old plants were infiltrated with 1 μM flg22 or mock (water) using a needleless syringe and collected at the indicated time points. Seedlings were submerged into liquid half-strength MS medium containing 100 μM MeJA or mock (water) for the indicated time period and, if required, transferred to new liquid half-strength MS medium containing 1 μM flg22 or mock. Total RNAs were isolated using TriFast (peqlab, Erlangen, Germany), followed by cDNA synthesis using superscript II (Life Technologies). Real-time PCR was performed using EvaGreen (Biotium, Hayward, CA, USA) on the iQ5 Multicolor Real-Time PCR Detection System (Bio-Rad, Munich, Germany) or the CFX Connect Real-Time PCR Detection System (Bio-Rad). Primers used are listed in Appendix Table S1. The following models were fit to the relative Ct value data compared to *Actin2*: $Ct_{gyr} = GY_{gy} + R_r + e_{gyr}$, where GY, genotype:treatment interaction and random factors; R, biological replicate; e, residual; $Ct_{ytr} = YT_{yt} + R_r + e_{ytr}$, where YT, treatment:time interaction and random factors; R, biological replicate; e, residual. The mean estimates of the fixed effects were used as the modeled relative Ct values, visualized as the relative log₂ expression values, and compared by two-tailed *t*-tests.

SA measurement

Leaves of 4- to 5-week-old plants were infiltrated with mock (water) or 1 μM flg22. Samples were harvested 9 h after the treatment and stored at –80°C. SA measurement was performed as described previously [60]. The following model was fit to log₂-transformed SA levels (pmol/g fresh weight): $SA_{gyr} = GY_{gy} + R_r + e_{gyr}$, where GY, genotype:treatment interaction and random factors; R, biological replicate; e, residual. The mean estimates of the fixed effects were compared by two-tailed *t*-tests.

Bacterial growth assay

Bacterial growth assays were performed essentially as described previously [54]. For measuring flg22-triggered immunity, bacterial suspensions were co-infiltrated with 1 μM flg22 into leaves of 4- to 5-week-old plants using a needleless syringe. For assessing effects of MeJA, 1 mM MeJA was sprayed onto 4- to 5-week-old plants shortly after infiltration of bacterial suspensions and 1 μM flg22. For assessing effects of temperature, 4- to 5-week-old plants were grown, infiltrated with bacterial suspension, and kept at 22 or 28°C

throughout the experiments. \log_{10} -transformed colony-forming units (cfu) per cm^2 leaf surface area were calculated, and the following model was fit to the data: $\text{CFU}_{\text{gyr}} = \text{GY}_{\text{gy}} + R_r + e_{\text{gyr}}$, where GY, genotype:treatment interaction and random factors; R, biological replicate; e, residual. Flg22-triggered immunity was calculated by subtracting the modeled bacterial titers in flg22-treated plants from those in the mock-treated plants.

Chromatin immunoprecipitation

Tissue fixation and chromatin immunoprecipitation were carried out as described [61] with some modifications. Briefly, 2-week-old seedlings grown in liquid half-strength MS medium supplemented with 1% sucrose were treated with 1 μM flg22 for 1 or 3 h. Untreated seedlings were also harvested. Alternatively, seedlings were treated with mock (water) or 100 μM MeJA for 3 h. After fixation in 1% formaldehyde solution, tissues were frozen in liquid nitrogen and stored at -80°C . Frozen tissues (~ 1 g) were ground in liquid nitrogen using a mortar and pestle and suspended in 3 ml of lysis buffer [50 mM Tris-HCl (pH 8.0), 2 mM EDTA, 150 mM NaCl, 1% Triton X-100, 50 μM MG132 (Sigma), and complete protease inhibitor cocktails (04693132001; Roche, Mannheim, Germany) or proteases inhibitor cocktail (P9599; Sigma)]. The suspension was sonicated twice on the Bioruptor Next Gen UCD-300 sonication system (Diagenode, Seraing, Belgium) for 10 min at 4°C , followed by centrifugation at $20,000 \times g$ for 10 min at 4°C . The supernatant was used as the starting material for chromatin immunoprecipitation using anti-GFP antibody (Ab290; Abcam, Cambridge, UK). Aliquots of the supernatant were kept as input samples. The samples were analyzed by quantitative PCR using primers listed in Appendix Table S1. The percentage of input values of the ChIP DNA was further normalized over the value obtained for the *Actin7* promoter (*AT5G09810*). Fold enrichment was then calculated by taking ratios between normalized results from wild-type plants and from MYC2-GFP plants. For statistical analysis, the following model was fit to \log_2 -transformed values of the normalized value data: $\text{Ct}_{\text{gyr}} = \text{GY}_{\text{gy}} + R_r + e_{\text{gyr}}$, where GY, genotype:treatment interaction and random factors; R, biological replicate; e, residual. The mean estimates of the fixed effects were compared by two-tailed *t*-tests.

Luciferase reporter assay

The WT *EDS5* promoter was amplified by PCR (PrimeSTAR HS DNA polymerase; Takara-Clontech) using pEDS5_F and pEDS5_R (with HindIII and BamHI restriction sites, respectively) listed in Appendix Table S1, designed as recommended by the In-Fusion HD cloning kit. For the *EDS5* promoter without the G box, two fragments were amplified by PCR using two sets of primers, pEDS5_F and pEDS5w/oGbox_R and pEDS5w/oGbox_F and pEDS5_R, respectively (Appendix Table S1) and then fused by PCR using pEDS5_F and pEDS5_R. These promoter sequences were cloned into HindIII/BamHI-digested pBI221-LUC using In-Fusion HD cloning kit (Takara-Clontech) to generate pBI221_pEDS5::LUC and pBI221_pEDS5w/oGbox::LUC. pENTR_MYC2 used in this study was obtained from Dr. Haitao Cui (Max Planck Institute for Plant Breeding Research, Germany) and recombined into pAM-PAT vector (35S promoter) with the Gateway LR clonase (Invitrogen) to obtain the pAM-PAT_MYC2 vector.

EDS5 promoter activity assays were performed by transient expression in *Arabidopsis* Col-0 protoplasts as described previously [62]. Protoplasts were transfected with pBI221_pEDS5::LUC or pBI221_pEDS5w/oGbox::LUC in the presence or absence of pAM-PAT_MYC2. The pPTRL plasmid [63] was included for normalization of transformation efficiency, which expresses *Renilla* luciferase under the 35S promoter. Nineteen hours post-transfection, protoplasts were harvested and luciferase assay was performed by Dual-Luciferase reporter assay system (Promega) and Centro LB 960 Microplate Luminometer (Berthold Technologies).

Phylogenetic analysis

The whole protein sequences of *A. thaliana*, *A. lyrata*, *C. rubella*, *C. grandiflora*, *E. salsugineum*, *B. rapa*, tomato, and rice were retrieved from Phytozome [64] and used for identification of putative orthologous groups using the OrthoMCL program [65]. The proteins belonging to the same group as *A. thaliana* *EDS5* were aligned using MUSCLE [66]. A maximum likelihood phylogenetic tree was constructed using the MEGA6 software [67]. To visualize conservation of G boxes, 500 bp upstream of the transcription start sites and 5'-UTRs of the *Brassicaceae* *EDS5* were retrieved from Phytozome and aligned using MUSCLE.

Accession numbers

The accession numbers for the genes discussed in this article are as follows: *AtActin2* (At3g18780), *AtDDE2* (AT5G42650), *AtCOI1* (AT2G39940), *AtMYC2* (AT1G32640), *AtMYC3* (AT5G46760), *AtMYC4* (At4G17880), *AtEDS5* (AT4G39030), *AtPAD4* (AT3G52430), *AtSID2* (At1g74710), *AtPR1* (At2G14610), *AlActin2* (342019), *AIE DS5* (490671), *AlPAD4* (938122), *EsActin2* (Thhalv10020949m), *EsEDS5* (Thhalv10024859m), *EsPAD4* (Thhalv10011112m), *CrActin2* (Carubv10013961m), *CrEDS5* (Carubv10004548m), *CrPAD4* (Carubv10016970m and Carubv10016967m), and *CrVSP2* (Carubv10001708 m).

Expanded View for this article is available online.

Acknowledgements

We thank Dr. Kei Hiruma (Nara Institute for Science and Technology) for the *myc2/jin-9* mutant, Dr. Philippe Reymond (University of Lausanne) for the *myc2 myc3 myc4* mutant, Dr. Hironaka Tsukagoshi (Meijo University) for the *p35S::MYC2-GFP* line, Dr. Haitao Cui (MPIPZ) for pENTR_MYC2, Dr. Nobutaka Mitsuda (AIST) for pPTRL, Dr. Thomas Griebel (MPIPZ) for help in SA measurement and ChIP experiments, Drs. Rainer Birkenbihl (MPIPZ) and Yasuomi Tada (Nagoya University) for help in ChIP experiments, and Drs. Fumiaki Katagiri and Jane Glazebrook (University of Minnesota) for critical reading of the manuscript. This work was supported by the Max Planck Society and Deutsche Forschungsgemeinschaft grant SFB670 (KT), and a Grant-in-Aid for the Japanese Society for the Promotion of Science (JSPS) Fellows (AM). AM was a recipient of a Postdoctoral Fellowship for Research Abroad from JSPS.

Author contributions

AM and KT conceived and designed the experiments. AM, TN, MCS-R, TMW, SA, and KT performed the experiments. AM and KT analyzed and discussed the data. DB contributed to generation of the plant materials. AM and KT wrote the manuscript.

Conflict of interest

The authors declare that they have no conflict of interest.

References

- Shoval O, Alon U (2010) SnapShot: network motifs. *Cell* 143: 326.e1
- Boller T, Felix G (2009) A renaissance of elicitors: perception of microbe-associated molecular patterns and danger signals by pattern-recognition receptors. *Annu Rev Plant Biol* 60: 379–406
- Jones JDC, Dangl JL (2006) The plant immune system. *Nature* 444: 323–329
- Tsuda K, Katagiri F (2010) Comparing signaling mechanisms engaged in pattern-triggered and effector-triggered immunity. *Curr Opin Plant Biol* 13: 459–465
- Macho Alberto P, Zipfel C (2014) Plant PRRs and the activation of innate immune signaling. *Mol Cell* 54: 263–272
- Heil M, Baldwin IT (2002) Fitness costs of induced resistance: emerging experimental support for a slippery concept. *Trends Plant Sci* 7: 61–67
- Alcázar R, Reymond M, Schmitz G, de Meaux J (2011) Genetic and evolutionary perspectives on the interplay between plant immunity and development. *Curr Opin Plant Biol* 14: 378–384
- Huot B, Yao J, Montgomery BL, He SY (2014) Growth-defense tradeoffs in plants: a balancing act to optimize fitness. *Mol Plant* 7: 1267–1287
- Smakowska E, Kong J, Busch W, Belkadir Y (2016) Organ-specific regulation of growth-defense tradeoffs by plants. *Curr Opin Plant Biol* 29: 129–137
- Boller T, He SY (2009) Innate immunity in plants: an arms race between pattern recognition receptors in plants and effectors in microbial pathogens. *Science* 324: 742–744
- Dou D, Zhou J-M (2012) Phytopathogen effectors subverting host immunity: different foes, similar battleground. *Cell Host Microbe* 12: 484–495
- Hua J (2013) Modulation of plant immunity by light, circadian rhythm, and temperature. *Curr Opin Plant Biol* 16: 406–413
- Glazebrook J (2005) Contrasting mechanisms of defense against biotrophic and necrotrophic pathogens. *Annu Rev Phytopathol* 43: 205–227
- Kim Y, Tsuda K, Igarashi D, Hillmer Rachel A, Sakakibara H, Myers Chad L, Katagiri F (2014) Mechanisms underlying robustness and tunability in a plant immune signaling network. *Cell Host Microbe* 15: 84–94
- Doares SH, Syrovets T, Weiler EW, Ryan CA (1995) Oligogalacturonides and chitosan activate plant defensive genes through the octadecanoid pathway. *Proc Natl Acad Sci USA* 92: 4095–4098
- von Malek B, van der Graaff E, Schneitz K, Keller B (2002) The *Arabidopsis* male-sterile mutant *dde2-2* is defective in the allene oxide synthase gene encoding one of the key enzymes of the jasmonic acid biosynthesis pathway. *Planta* 216: 187–192
- Staswick PE (2002) Jasmonate response locus JAR1 and several related *Arabidopsis* genes encode enzymes of the firefly luciferase superfamily that show activity on jasmonic, salicylic, and indole-3-acetic acids in an assay for adenylation. *Plant Cell Online* 14: 1405–1415
- Staswick PE (2004) The oxylipin signal jasmonic acid is activated by an enzyme that conjugates it to isoleucine in *Arabidopsis*. *Plant Cell Online* 16: 2117–2127
- Xie DX, Feys BF, James S, Nieto-Rostro M, Turner JG (1998) COI1: an *Arabidopsis* gene required for jasmonate-regulated defense and fertility. *Science* 280: 1091–1094
- Katsir L, Schilmiller AL, Staswick PE, He SY, Howe GA (2008) COI1 is a critical component of a receptor for jasmonate and the bacterial virulence factor coronatine. *Proc Natl Acad Sci USA* 105: 7100–7105
- Sheard LB, Tan X, Mao H, Withers J, Ben-Nissan G, Hinds TR, Kobayashi Y, Hsu F-F, Sharon M, Browse J et al (2010) Jasmonate perception by inositol-phosphate-potentiated COI1–JAZ co-receptor. *Nature* 468: 400–405
- Song S, Qi T, Wasternack C, Xie D (2014) Jasmonate signaling and crosstalk with gibberellin and ethylene. *Curr Opin Plant Biol* 21: 112–119
- Wasternack C, Hause B (2013) Jasmonates: biosynthesis, perception, signal transduction and action in plant stress response, growth and development. An update to the 2007 review in *Annals of Botany*. *Ann Bot* 111: 1021–1058
- Seyfferth C, Tsuda K (2014) Salicylic acid signal transduction: the initiation of biosynthesis, perception and transcriptional reprogramming. *Front Plant Sci* 5: 697
- Tsuda K, Sato M, Glazebrook J, Cohen JD, Katagiri F (2008) Interplay between MAMP-triggered and SA-mediated defense responses. *Plant J* 53: 763–775
- Wildermuth MC, Dewdney J, Wu G, Ausubel FM (2001) Isochorismate synthase is required to synthesize salicylic acid for plant defence. *Nature* 414: 562–565
- Jirage D, Tootle TL, Reuber TL, Frost LN, Feys BJ, Parker JE, Ausubel FM, Glazebrook J (1999) *Arabidopsis thaliana* PAD4 encodes a lipase-like gene that is important for salicylic acid signaling. *Proc Natl Acad Sci USA* 96: 13583–13588
- Nawrath C (2002) EDS5, an essential component of salicylic acid-dependent signaling for disease resistance in *Arabidopsis*, is a member of the mate transporter family. *Plant Cell Online* 14: 275–286
- Nawrath C, Metraux JP (1999) Salicylic acid induction-deficient mutants of *Arabidopsis* express PR-2 and PR-5 and accumulate high levels of camalexin after pathogen inoculation. *Plant Cell* 11: 1393–1404
- Serrano M, Wang B, Aryal B, Garcion C, Abou-Mansour E, Heck S, Geisler M, Mauch F, Nawrath C, Metraux JP (2013) Export of salicylic acid from the chloroplast requires the multidrug and toxin extrusion-like transporter EDS5. *Plant Physiol* 162: 1815–1821
- Vlot AC, Dempsey DMA, Klessig DF (2009) Salicylic acid, a multifaceted hormone to combat disease. *Annu Rev Phytopathol* 47: 177–206
- Zhang YL, Goritschnig S, Dong XN, Li X (2003) A gain-of-function mutation in a plant disease resistance gene leads to constitutive activation of downstream signal transduction pathways in suppressor of *npr1-1*, constitutive 1. *Plant Cell* 15: 2636–2646
- Mauch F, Mauch-Mani B, Gaille C, Kull B, Haas D, Reimann C (2001) Manipulation of salicylate content in *Arabidopsis thaliana* by the expression of an engineered bacterial salicylate synthase. *Plant J* 25: 67–77
- Saleh A, Withers J, Mohan R, Marques J, Gu YN, Yan SP, Zavaliev R, Nomoto M, Tada Y, Dong XN (2015) Posttranslational modifications of the master transcriptional regulator NPR1 enable dynamic but tight control of plant immune responses. *Cell Host Microbe* 18: 169–182
- Pieterse CMJ, Van der Does D, Zamioudis C, Leon-Reyes A, Van Wees SCM (2012) Hormonal modulation of plant immunity. *Annu Rev Cell Dev Biol* 28: 489–521
- Mine A, Sato M, Tsuda K (2014) Toward a systems understanding of plant-microbe interactions. *Front Plant Sci* 5: 423
- Spoel SH, Johnson JS, Dong X (2007) Regulation of tradeoffs between plant defenses against pathogens with different lifestyles. *Proc Natl Acad Sci USA* 104: 18842–18847
- Mur LAJ (2005) The outcomes of concentration-specific interactions between salicylate and jasmonate signaling include synergy, antagonism, and oxidative stress leading to cell death. *Plant Physiol* 140: 249–262

39. Tsuda K, Mine A, Bethke G, Igarashi D, Botanga CJ, Tsuda Y, Glazebrook J, Sato M, Katagiri F (2013) Dual regulation of gene expression mediated by extended MAPK activation and salicylic acid contributes to robust innate immunity in *Arabidopsis thaliana*. *PLoS Genet* 9: e1004015
40. Kazan K, Manners JM (2013) MYC2: the master in action. *Mol Plant* 6: 686–703
41. Abe H, YamaguchiShinozaki K, Urao T, Iwasaki T, Hosokawa D, Shinozaki K (1997) Role of *Arabidopsis* MYC and MYB homologs in drought- and abscisic acid-regulated gene expression. *Plant Cell* 9: 1859–1868
42. O'Connor TR, Dyreson C, Wyrick JJ (2005) Athena: a resource for rapid visualization and systematic analysis of *Arabidopsis* promoter sequences. *Bioinformatics* 21: 4411–4413
43. Fernández-Calvo P, Chini A, Fernández-Barbero G, Chico J-M, Gimenez-Ibanez S, Geerinck J, Eeckhout D, Schweizer F, Godoy M, Franco-Zorrilla JM et al (2011) The *Arabidopsis* bHLH transcription factors MYC3 and MYC4 are targets of JAZ repressors and act additively with MYC2 in the activation of jasmonate responses. *Plant Cell* 23: 701–715
44. Alcázar R, Parker JE (2011) The impact of temperature on balancing immune responsiveness and growth in *Arabidopsis*. *Trends Plant Sci* 16: 666–675
45. Mittal S, Davis KR (1995) Role of the phytotoxin coronatine in the infection of *Arabidopsis thaliana* by *Pseudomonas syringae* pv tomato. *Mol Plant Microbe Interact* 8: 165–171
46. Koenig D, Weigel D (2015) Beyond the thale: comparative genomics and genetics of *Arabidopsis* relatives. *Nat Rev Genet* 16: 285–298
47. Wagner S, Stuttmann J, Rietz S, Guerois R, Brunstein E, Bautor J, Niefind K, Parker Jane E (2013) Structural basis for signaling by exclusive EDS1 heteromeric complexes with SAG101 or PAD4 in plant innate immunity. *Cell Host Microbe* 14: 619–630
48. Alon U (2007) Network motifs: theory and experimental approaches. *Nat Rev Genet* 8: 450–461
49. Mangan S, Alon U (2003) Structure and function of the feed-forward loop network motif. *Proc Natl Acad Sci USA* 100: 11980–11985
50. Zheng XY, Spivey NW, Zeng WQ, Liu PP, Fu ZQ, Klessig DF, He SY, Dong XN (2012) Coronatine promotes *Pseudomonas syringae* virulence in plants by activating a signaling cascade that inhibits salicylic acid accumulation. *Cell Host Microbe* 11: 587–596
51. Wang J, Shine MB, Gao QM, Navarre D, Jiang W, Liu C, Chen Q, Hu G, Kachroo A (2014) Enhanced disease susceptibility 1 mediates pathogen resistance and virulence function of a bacterial effector in soybean. *Plant Physiol* 165: 1269–1284
52. Bhattacharjee S, Halane MK, Kim SH, Gassmann W (2011) Pathogen effectors target *Arabidopsis* EDS1 and alter its interactions with immune regulators. *Science* 334: 1405–1408
53. Slotte T, Hazzouri KM, Ågren JA, Koenig D, Maumus F, Guo Y-L, Steige K, Platts AE, Escobar JS, Newman LK et al (2013) The *Capsella rubella* genome and the genomic consequences of rapid mating system evolution. *Nat Genet* 45: 831–835
54. Tsuda K, Sato M, Stoddard T, Glazebrook J, Katagiri F (2009) Network properties of robust immunity in plants. *PLoS Genet* 5: e1000772
55. Anderson JP (2004) Antagonistic interaction between abscisic acid and jasmonate-ethylene signaling pathways modulates defense gene expression and disease resistance in *Arabidopsis*. *Plant Cell Online* 16: 3460–3479
56. Zipfel C, Robatzek S, Navarro L, Oakeley EJ, Jones JDG, Felix G, Boller T (2004) Bacterial disease resistance in *Arabidopsis* through flagellin perception. *Nature* 428: 764–767
57. Chen H, Xue L, Chintamanani S, Germain H, Lin H, Cui H, Cai R, Zuo J, Tang X, Li X et al (2009) Ethylene insensitive3 and ethylene insensitive3-like1 repress salicylic acid induction deficient2 expression to negatively regulate plant innate immunity in *Arabidopsis*. *Plant Cell Online* 21: 2527–2540
58. Guo HS, Fei JF, Xie Q, Chua NH (2003) A chemical-regulated inducible RNAi system in plants. *Plant J* 34: 383–392
59. Shimada TL, Shimada T, Hara-Nishimura I (2010) A rapid and non-destructive screenable marker, FAST, for identifying transformed seeds of *Arabidopsis thaliana*. *Plant J* 61: 519–528
60. Villajuana-Bonequi M, Elrouby N, Nordström K, Griebel T, Bachmair A, Coupland G (2014) Elevated salicylic acid levels conferred by increased expression of isochorismate synthase 1 contribute to hyperaccumulation of SUMO1 conjugates in the *Arabidopsis* mutant early in short days 4. *Plant J* 79: 206–219
61. Yamaguchi N, Winter CM, Wu M-F, Kwon CS, William DA, Wagner D (2014) Protocol: chromatin immunoprecipitation from *Arabidopsis* tissues. *Arabidopsis Book* 12: e0170
62. Yoo S-D, Cho Y-H, Sheen J (2007) *Arabidopsis* mesophyll protoplasts: a versatile cell system for transient gene expression analysis. *Nat Protoc* 2: 1565–1572
63. Ohta M, Ohme-Takagi M, Shinshi H (2000) Three ethylene-responsive transcription factors in tobacco with distinct transactivation functions. *Plant J* 22: 29–38
64. Goodstein DM, Shu S, Howson R, Neupane R, Hayes RD, Fazo J, Mitros T, Dirks W, Hellsten U, Putnam N et al (2011) Phytozome: a comparative platform for green plant genomics. *Nucleic Acids Res* 40: D1178–D1186
65. Li L, Stoekert CJ, Roos DS (2003) OrthoMCL: identification of ortholog groups for eukaryotic genomes. *Genome Res* 13: 2178–2189
66. Edgar RC (2004) MUSCLE: multiple sequence alignment with high accuracy and high throughput. *Nucleic Acids Res* 32: 1792–1797
67. Tamura K, Stecher G, Peterson D, Filipiński A, Kumar S (2013) MEGA6: molecular evolutionary genetics analysis version 6.0. *Mol Biol Evol* 30: 2725–2729